doi:10.3772/j.issn.1006-6748.2018.02.004

Backstepping sliding mode control with self recurrent wavelet neural network observer for a novel coaxial twelve-rotor UAV①

Qiao Guanyu(乔冠宇)* **, Peng Cheng②*
(* Changchun Institute of Optics, Fine Mechanics and Physics, Chinese Academy of Sciences, Changchun 130033, P. R. China)
(** University of Chinese Academy of Sciences, Beijing 100039, P. R. China)

Abstract

The robust attitude control for a novel coaxial twelve-rotor UAV which has much greater payload capacity, higher drive capability and damage tolerance than a quad-rotor UAV is studied. Firstly, a dynamical and kinematical model for the coaxial twelve-rotor UAV is designed. Considering model uncertainties and external disturbances, a robust backstepping sliding mode control (BSMC) with self recurrent wavelet neural network (SRWNN) method is proposed as the attitude controller for the coaxial twelve-rotor. A combinative algorithm of backstepping control and sliding mode control has simplified design procedures with much stronger robustness benefiting from advantages of both controllers. SRWNN as the uncertainty observer is able to estimate the lumped uncertainties effectively. Then the uniformly ultimate stability of the twelve-rotor system is proved by Lyapunov stability theorem. Finally, the validity of the proposed robust control method adopted in the twelve-rotor UAV under model uncertainties and external disturbances are demonstrated via numerical simulations and twelve-rotor prototype experiments.

Key words: coaxial twelve-rotor UAV, backstepping sliding mode control (BSMC), self recurrent wavelet neural network (SRWNN), model uncertainties, external disturbances

0 Introduction

Recently, a quad-rotor UAV as the rotary wing UAV has evoked a great interest in the automatic control community due to its simple mechanical structure, attractive vertical take-off and landing capability[1], and their wide applications like surveillance, building exploration and information collection[2]. However, there are many difficult problems in controlling quad-rotor UAV because of the inevitable uncertainties in the practical situations[3]. Thus, the robust control problem has been increasingly considered for quad-rotor with model uncertainties and external disturbances. Mohammadi et al.[4] used a model reference adaptive control technique to control a quad-rotor under various conditions with parametric and non-parametric uncertainties in the model. Accurate simulation including empirical dynamic model of battery, sensors, and actuators was performed to validate the stability of the closed loop system. A simple robust quad-rotor controller[5] was provided using linear matrix inequalities to synthesize controller gains. The controller is based on approximate feedback linearization considering dynamic external disturbances, inexact nonlinearity cancellation, multiplicative actuator uncertainty and saturated integrators. A super twisting algorithm was applied to a quadrotor in Ref. [6] in order to ensure robustness against bounded disturbances. The fuzzy inference mechanism was proposed to help to estimate the upper bound of lumped uncertainty in quadrotor[7].

The above robust control methods are all based on the inherent structure of quad-rotor which has weak drive capability and remarkable underactuated characteristic. Therefore, this paper develops a novel coaxial twelve-rotor UAV with a new configuration. It is designed with twelve rotors that are arranged as six counter-rotating offset pairs mounted at the ends of six carbon fiber arms in a non-planar symmetrical configuration. Each rotor rotating plane is fixed as the tilt angle with the body plane. The six groups of the rotor speed in the non-planar are able to provide independently ad-

① Supported by the National Natural Science Foundation of China (No. 11372309, 61304017), Science and Technology Development Plan Key Project of Jilin Province (No. 20150204074GX) and the Science and Technology Special Fund Project of Provincial Academy Cooperation (No. 2017SYHZ00024).

② To whom correspondence should be addressed. E-mail: litianjinorc@126.com

Received on Aug. 21, 2017

justed forces and moments in the three axises. This unique design can realize the decoupling on movement and attitude and eliminate the underactuated characteristic. In the meantime, the yaw attitude control ability is greatly improved due to the fact that the yaw movement provided by the reactive torque in quad-rotor is replaced by the lift force in twelve-rotor. Therefore, the twelve-rotor UAV offers advantages about markedly increased drive capability and greater resistant to disturbance, which represents greater utility in practical applications. Furthermore, the twelve-rotor has stronger damage tolerance to remain stable flight when some of rotors are broken.

On account of model uncertainties of the twelve-rotor and external disturbances, a robust backstepping sliding mode control (BSMC) with self recurrent wavelet neural network (SRWNN) is proposed as the attitude controller. The backstepping sliding mode controller has great inherent insensitivity and strong robustness against disturbances. SRWNN as the uncertainties observer combines the properties of attractor dynamics of recurrent neural network[8] and the good convergence of wavelet neural network[9]. SRWNN can store the past information of the network and adapt rapidly to sudden changes of the control environment because it has a mother wavelet layer composed of self-feedback neurons[10]. Finally, the good attitude control performance of BSMC with SRWNN method is demonstrated by simulations in the case where the inertia matrix uncertainties as model uncertainties and time-varying external disturbance are taken into account. In the meantime, the validity of the proposed method applied to the coaxial twelve-rotor is corroborated by prototype experiments.

1 Dynamic model of coaxial twelve-rotor UAV

The scheme of the coaxial twelve-rotor UAV is shown in Fig. 1. Rotors of 1, 3, 5, 8, 10 rotate counterclockwise, while the other rotors rotate clockwise. Every two coaxial rotors have axis coincidence and form the same angle $\gamma(0 < \gamma < 90°)$ with the body plane. There are two main reference frames defined to express the dynamics of twelve-rotor. Both the earth-fixed inertial frame $E = \{Ox_e y_e z_e\}$ and the body-fixed frame $B = \{Ox_b y_b z_b\}$ are fixed at the centre of the aircraft. The thrust f_i and reactive torque τ_i produced by the ith rotor are expressed as

$$\begin{aligned} f_i &= k_i \Omega_i^2 \\ \tau_i &= k_{\tau i} \Omega_i^2 \end{aligned} \tag{1}$$

where $i = 1, 2, \cdots 12$ represents the rotor number, k_i and $k_{\tau i}$ are the thrust coefficient and reactive torque coefficient respectively, and $\boldsymbol{\Omega}_i$ expresses the ith rotor speed.

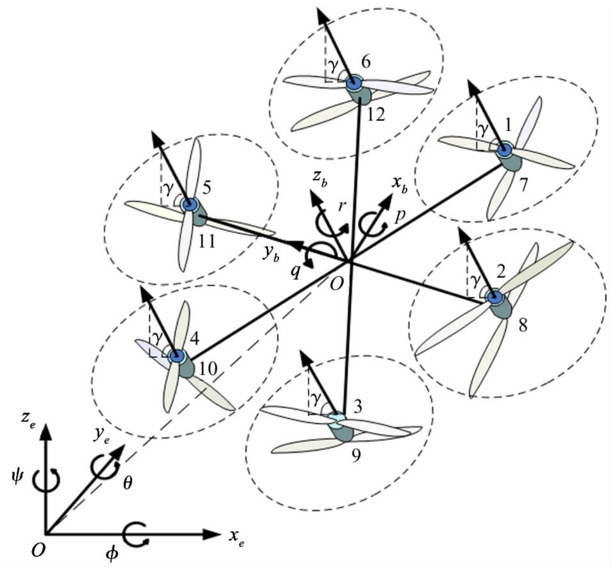

Fig. 1 The scheme of the coaxial twelve-rotor UAV

The position vector $\boldsymbol{P}_i \in R^3$, $i = 1, 2, \cdots, 12$ of the ith rotor in body-fixed frame B is defined as follow

$$\begin{aligned}
\boldsymbol{P}_1 &= \boldsymbol{P}_7 = \left[\frac{\sqrt{3}}{2} \quad -\frac{1}{2} \quad 0\right]^{\mathrm{T}} \\
\boldsymbol{P}_2 &= \boldsymbol{P}_8 = [0 \quad -1 \quad 0]^{\mathrm{T}} \\
\boldsymbol{P}_3 &= \boldsymbol{P}_9 = \left[-\frac{\sqrt{3}}{2} \quad -\frac{1}{2} \quad 0\right]^{\mathrm{T}} \\
\boldsymbol{P}_4 &= \boldsymbol{P}_{10} = \left[-\frac{\sqrt{3}}{2} \quad \frac{1}{2} \quad 0\right]^{\mathrm{T}} \\
\boldsymbol{P}_5 &= \boldsymbol{P}_{11} = [0 \quad 1 \quad 0]^{\mathrm{T}} \\
\boldsymbol{P}_6 &= \boldsymbol{P}_{12} = \left[\frac{\sqrt{3}}{2} \quad \frac{1}{2} \quad 0\right]^{\mathrm{T}}
\end{aligned} \tag{2}$$

Direction vector $\boldsymbol{D}_i \in R^3$, $i = 1, 2, \cdots, 12$ of the ith rotor in body-fixed frame B is defined as follows

$$\begin{aligned}
\boldsymbol{D}_1 &= \boldsymbol{D}_4 = \boldsymbol{D}_7 = \boldsymbol{D}_{10} = \left[\frac{1}{2}\sin\gamma \quad \frac{\sqrt{3}}{2}\sin\gamma \quad \cos\gamma\right]^{\mathrm{T}} \\
\boldsymbol{D}_2 &= \boldsymbol{D}_5 = \boldsymbol{D}_8 = \boldsymbol{D}_{11} = [-\sin\gamma \quad 0 \quad \cos\gamma]^{\mathrm{T}} \\
\boldsymbol{D}_3 &= \boldsymbol{D}_6 = \boldsymbol{D}_9 = \boldsymbol{D}_{12} = \left[\frac{1}{2}\sin\gamma \quad -\frac{\sqrt{3}}{2}\sin\gamma \quad \cos\gamma\right]^{\mathrm{T}}
\end{aligned} \tag{3}$$

Then, resultant F in body-fixed frame B is written as

$$F = \sum_{i=1}^{12} (P_i \cdot f_i) \tag{4}$$

and resultant moment M in body-fixed frame B as

$$\boldsymbol{M} = \sum_{i=1}^{12} (P_i \times f_i l + D_i \cdot \tau_i) \tag{5}$$

Owing to the twelve-rotor treated as a symmetrical rigid body with six degrees of freedom, the nonlinear dynamics can be derived using Newton-Euler formulas. The rotational dynamic equations can be obtained by

$$(\boldsymbol{J} + \Delta\boldsymbol{J}) \cdot \dot{\boldsymbol{\omega}} = - sk(\boldsymbol{\omega}) \cdot (\boldsymbol{J} + \Delta\boldsymbol{J}) \cdot \boldsymbol{\omega} + \boldsymbol{M} \tag{6}$$

where $\boldsymbol{J} = diag(I_x, I_y, I_z)$ is the moment of inertia, $\Delta\boldsymbol{J} = diag(\Delta I_x, \Delta I_y, \Delta I_z)$ treated as the inertia matrix uncertainty caused by the change in mass properties. $\boldsymbol{\omega} = [p, q, r]^{\mathrm{T}}$ is the angle velocity on B. $sk(\boldsymbol{\omega})$ as skew-symmetric matrix is denoted by

$$sk(\boldsymbol{\omega}) = \begin{bmatrix} 0 & -r & q \\ r & 0 & -p \\ -q & p & 0 \end{bmatrix} \tag{7}$$

Due to external disturbances, in the general case of small attitude, the rotational kinematics equation can be facilitated as follows

$$\begin{bmatrix} \ddot{\phi} \\ \ddot{\theta} \\ \ddot{\psi} \end{bmatrix} = \begin{bmatrix} M_x/(I_x + \Delta I_x) + \tau_{dx} \\ M_y/(I_y + \Delta I_y) + \tau_{dy} \\ M_z/(I_z + \Delta I_z) + \tau_{dz} \end{bmatrix} \tag{8}$$

$\boldsymbol{\tau}_d = [\tau_{dx} \quad \tau_{dy} \quad \tau_{dy}]$ denotes external disturbances, the attitude is expressed by Euler angles $\boldsymbol{\eta} = [\phi \quad \theta \quad \psi]^{\mathrm{T}}$ and the resultant moment is $\boldsymbol{M} = [M_x \quad M_y \quad M_z]^{\mathrm{T}}$.

The translational model calculated by the Newton-Euler equation is derived as

$$m\frac{d\boldsymbol{V}}{dt} = m(\frac{\delta \boldsymbol{V}}{\delta t} + \omega \times \boldsymbol{V}) = \boldsymbol{F} + \Delta\boldsymbol{F} + \boldsymbol{R}^{-1}G \tag{9}$$

where $\boldsymbol{V} = [u, v, w]^{\mathrm{T}}$ denotes the velocity with respect to B, $\Delta\boldsymbol{F}$ is treated as the neglectful aerodynamic force. The rotation matrix map vector $\boldsymbol{R}$ from the body-fixed frame B to the inertial frame E is expressed as

$$\boldsymbol{R} = \begin{bmatrix} \cos\psi\cos\theta & -\sin\psi\cos\phi + \cos\psi\sin\theta\sin\phi & \sin\psi\sin\phi + \cos\psi\sin\theta\cos\phi \\ \sin\psi\cos\theta & \cos\psi\cos\phi + \cos\psi\sin\theta\sin\phi & -\cos\psi\sin\phi + \sin\psi\sin\theta\cos\phi \\ -\sin\theta & \cos\theta\sin\phi & \cos\theta\cos\phi \end{bmatrix} \tag{10}$$

Moreover, the relationship between velocity $\boldsymbol{V}$ and inertial translational position $\boldsymbol{P} = [x \quad y \quad z]^{\mathrm{T}}$ is described as

$$\dot{\boldsymbol{P}} = \boldsymbol{R} \cdot \boldsymbol{V} \tag{11}$$

Therefore, the translational dynamic model is obtained as follows

$$\begin{bmatrix} \ddot{x} \\ \ddot{y} \\ \ddot{z} \end{bmatrix} = \frac{1}{m}\begin{bmatrix} F_x\cos\psi\cos\theta + F_y(\cos\psi\sin\theta\cos\phi - \sin\psi\cos\phi) + F_z(\cos\psi\sin\theta\cos\phi + \sin\psi\sin\phi) \\ F_x\sin\psi\cos\theta + F_y(\cos\psi\sin\theta\sin\phi + \cos\psi\cos\phi) + F_z(\sin\psi\sin\theta\cos\phi - \cos\psi\sin\phi) \\ -F_x\sin\theta + F_y\sin\phi\cos\psi + F_z\cos\theta\cos\phi - mg \end{bmatrix} \tag{12}$$

2 Robust attitude control of the twelve-rotor

Considering the inevitable model uncertainties and external disturbances, BSMC with SRWNN method is exploited as the attitude controller of the twelve-rotor. The attitude control block diagram is depicted in Fig. 2, in which the attitude control system is divided into three channels, that is, roll channel, pitch channel, and yaw channel. Each channel is controlled by BSMC with SRWNN separately.

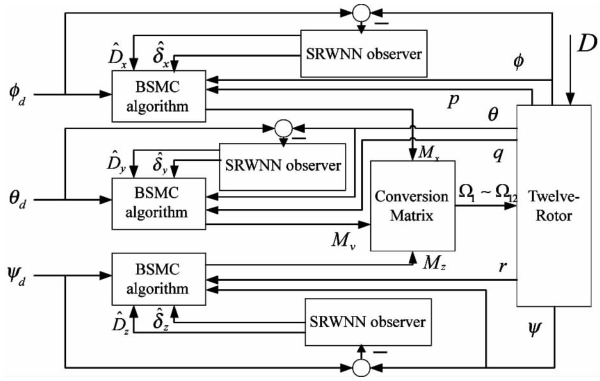

Fig. 2 The attitude control block diagram of the twelve-rotor UAV

Take the roll channel of the twelve-rotor as an example, which is described as

$$\begin{aligned} \dot{x}_1 &= x_2 \\ \dot{x}_2 &= M_x/I_x + D_x \end{aligned} \tag{13}$$

where x_1 is the roll angle, x_2 is the roll angle velocity. $D_x = \tau_{dx} + f_x$ denotes the lumped uncertainties in the roll channel, where τ_{dx} as the external disturbance is bound, and $f_x = -\Delta I_x M_x/[(I_x + \Delta I_x) \cdot I_x]$ expresses the model uncertainty.

Firstly, the roll angle tracking error is defined as

$$z_1 = x_{1d} - x_1 \tag{14}$$

with x_{1d} as the desired roll angle. Define the stabilizing function as follows

$$c_1 = \alpha_1 z_1 \tag{15}$$

with α_1 as a positive constant. The roll angle velocity tracking error is denoted as $z_2 = x_2 - \dot{x}_{1d} - c_1$. Choose the first Lyapunov function as $V_1 = z_1^2/2$, then the derivative of V_1 is

$$\dot{V}_1 = z_1(\dot{x}_{1d} - x_2) = -z_1 z_2 - \alpha z_1^2 \tag{16}$$

Due to the fact that the derivative of z_2 can be expressed as

$$\begin{aligned} \dot{z}_2 &= \dot{x}_2 - \ddot{x}_{1d} - \alpha\dot{z}_1 \\ &= M_x/I_x + D_x - \ddot{x}_{1d} + \alpha(z_2 + \alpha z_1) \end{aligned} \tag{17}$$

Therefore, the second Lyapunov function is chosen by

$$V_2 = V_1 + \frac{1}{2}s^2 \tag{18}$$

and where

$$s = kz_1 + z_2 \tag{19}$$

with k is a positive constant. Thereby, it can be derived that

$$\begin{aligned} \dot{V}_2 &= \dot{V}_1 + s\dot{s} = -z_1z_2 - \alpha z_1^2 + s(kz_1 + z_2) \\ &= -z_1z_2 - \alpha z_1^2 + s[(k-\alpha)\dot{z}_1 + M_x/I_x + D_x - \ddot{x}_{1d}] \end{aligned} \tag{20}$$

Then, in an attempt to estimate the lumped uncertainty D_x, the SRWNN observer is exploited, which consists of four layers: an input layer, a mother wavelet layer, a product layer and an output layer, as shown in Fig. 3. The mother wavelets are chosen as the first derivative of a Gaussian function. The weights a_k, $m_{jk}, d_{jk}, \theta_{jk}$, w_j will be trained online by the adaptation laws based on Lyapunov stability analysis.

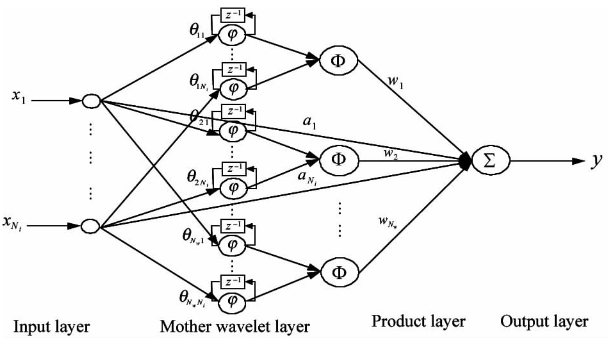

Fig. 3 The structure of SRWNN

Define the SRWNN uncertainty observer as follow

$$\hat{D}_x = \hat{\boldsymbol{W}}^{\mathrm{T}}\hat{\boldsymbol{\Phi}}(x, \hat{\boldsymbol{M}}, \hat{\boldsymbol{D}}, \hat{\boldsymbol{\Theta}}) + \hat{\boldsymbol{A}}^{\mathrm{T}}\boldsymbol{X} \tag{21}$$

where $\boldsymbol{X} = [z_1, \dot{z}_1]^{\mathrm{T}}$ denotes the input of SRWNN. $\hat{\boldsymbol{W}}$, $\hat{\boldsymbol{M}}, \hat{\boldsymbol{D}}, \hat{\boldsymbol{\Theta}}, \hat{\boldsymbol{A}}$ express the estimation vector of $m_{jk}, d_{jk}, \theta_{jk}, a_k$, respectively. The product layer is derived as $\hat{\boldsymbol{\Phi}} = \hat{\boldsymbol{\Phi}}(x, \hat{\boldsymbol{M}}, \hat{\boldsymbol{D}}, \hat{\boldsymbol{\Theta}})$. In view of the universal approximation theorem, the estimated error $\tilde{D}_x = D_x - \hat{D}_x$ can be rewritten as

$$\tilde{D}_x = \tilde{\boldsymbol{W}}^{\mathrm{T}}\hat{\boldsymbol{\Phi}} + \tilde{\boldsymbol{M}}^{\mathrm{T}}\boldsymbol{E}\hat{\boldsymbol{W}} + \tilde{\boldsymbol{D}}^{\mathrm{T}}\boldsymbol{C}\hat{\boldsymbol{W}} + \tilde{\boldsymbol{\Theta}}^{\mathrm{T}}\boldsymbol{G}\hat{\boldsymbol{W}} + \tilde{\boldsymbol{A}}^{\mathrm{T}}\boldsymbol{X} + \boldsymbol{\Delta} \tag{22}$$

with the expansion of $\tilde{\boldsymbol{\Phi}}$ in Taylor series, where

$$\begin{aligned} E &= [\partial\Phi_1/\partial M,\ \partial\Phi_2\partial M, \cdots, \partial\Phi_{N_w}/\partial M] \mid_{M=\hat{M}} \\ C &= [\partial\Phi_1/\partial D,\ \partial\Phi_2/\partial D, \cdots, \partial\Phi_{N_w}/\partial D] \mid_{D=\hat{D}} \\ G &= [\partial\Phi_1/\partial\Theta,\ \partial\Phi_2/\partial\Theta, \cdots, \partial\Phi_{N_w}/\partial\Theta] \mid_{\Theta=\Theta} \end{aligned} \tag{23}$$

and $\tilde{W} = W^* - \hat{W}$, $\tilde{\boldsymbol{\Phi}} = \boldsymbol{\Phi}^* - \hat{\boldsymbol{\Phi}}$, $\tilde{A} = A^* - \hat{A}$. H denotes the higher-order terms. Δ represents an approximation error term and $|\Delta| \leqslant P$.

Then, the Lyapunov candidate is chosen as

$$V_3 = V_2 + \frac{1}{2\eta_1}\tilde{W}^{\mathrm{T}}\tilde{W} + \frac{1}{2\eta_2}\tilde{M}^{\mathrm{T}}\tilde{M} + \frac{1}{2\eta_3}\tilde{D}^{\mathrm{T}}\tilde{D} + \frac{1}{2\eta_4}\tilde{\Theta}^{\mathrm{T}}\tilde{\Theta} + \frac{1}{2\eta_5}\tilde{P}^{\mathrm{T}}\tilde{P} + \frac{1}{2\eta_6}\tilde{A}^{\mathrm{T}}\tilde{A} \tag{24}$$

where $\eta_1, \eta_2, \eta_3, \eta_4, \eta_5, \eta_6$ are all positive constants. Therefore, the BSMC with SRWNN control law U_x is designed by

$$\begin{aligned} U_x &= M_x \\ &= I_x[-(k-\alpha)\dot{z}_1 + \ddot{x}_{1d} - \gamma s - h\,\mathrm{sgn}(s) - \hat{D}_x \\ &\quad - \hat{\boldsymbol{P}}\,\mathrm{sgn}(s)] \end{aligned} \tag{25}$$

with γ and h as positive constants. The adaptive laws for the SRWNN observer and the approximation error bound are given as follows

$$\begin{aligned} &\dot{\hat{W}} = -\dot{\tilde{W}} = \eta_1 s\,\hat{\boldsymbol{\Phi}} \quad \dot{\hat{W}} = -\dot{\tilde{W}} = \eta_2 sE\,\hat{W} \\ &\dot{\hat{D}} = -\dot{\tilde{D}} = \eta_3 sC\,\hat{W} \quad \dot{\hat{\Theta}} = -\dot{\tilde{\Theta}} = \eta_4 sG\,\hat{W} \\ &\dot{\hat{A}} = -\dot{\tilde{A}} = \eta_6 sX \quad \dot{\hat{P}} = -\dot{\tilde{P}} = \eta_5 |s| \end{aligned} \tag{26}$$

Then, the derivative of V_3 can be written as

$$\begin{aligned} \dot{V}_3 &= -z_1z_2 - \alpha z_1^2 - \gamma s^2 - h|s| + s\Delta - P|s| \\ &\leqslant -z_1z_2 - \alpha z_1^2 - \gamma s^2 - h|s| \end{aligned} \tag{27}$$

Based on Barbalat's lemma[11], it is shown that $\dot{V}_3 \leqslant 0$ in the case where $\gamma(\alpha - k) - \frac{1}{4} > 0$. Therefore, the twelve-rotor control system in the roll channel can be asymptotically stable in the present of above condition under model uncertainties and external disturbances. Furthermore, the attitude control system in pitch channel and yaw channel based on the proposed method have the same design procedure, which is no longer description for the sake of simplicity.

3 Numerical simulations results

The attitude control simulations of the coaxial twelve-rotor UAV between BSMC with SRWNN method and BSMC method are carried out to demonstrate the validity and robustness of the proposed method in the case of model uncertainties and external disturbances. The parameters of dynamic model in simulations are taken from the twelve-rotor prototype, as listed in Table 1.

Table 1 The parameters of the eight-rotor prototype

Parameters	Values
Mass (m)	4.45kg
Distance between rotor and the centre (l)	0.5m
Moment of inertia to x-axis (I_x)	2.6×10^{-2} Nm/s^2
Moment of inertia to y-axis (I_y)	2.6×10^{-2} Nm/s^2
Moment of inertia to z-axis (I_z)	4.2×10^{-2} Nm/s^2
Thrust factor (k_1)	54.2×10^{-6} Ns^2
Drag factor (k_2)	1.1×10^{-6} Nm/s^2

Assume the initial attitude angles as $\eta_0 = [0 \quad 0 \quad 0]^T$ degree, and the desired attitude angles as $\eta_d = [12\cos(t) \quad 12\cos(t) \quad 30\cos(t)]^T$ degree. An uncertainty of -30% in the inertia matrix is given as the model uncertainties. The time-varying external disturbance that acts on the three attitudes is assumed as $\tau_d = 0.2\sin(0.5t)$. Furthermore, parameters of BSMC are set as $\alpha_x = 10$, $k_x = 0.5$, $\gamma_x = 18$, $h_x = 1$, $\alpha_y = 14$, $k_y = 0.5$, $\gamma_y = 21$, $h_y = 3$, $\alpha_z = 12$, $k_z = 0.5$, $h_z = 1$. What's more, learning rates of SRWNN observer are given as $\eta_1 = \eta_2 = \eta_3 = \eta_4 = \eta_6 = 10$, $\eta_5 = 0.4$ by the trial and error.

The three attitude compared simulations between BSMC with SRWNN and BSMC method are operated under model uncertainties and time-varying external disturbance, as described in Fig. 4, Fig. 5 and Fig. 6.

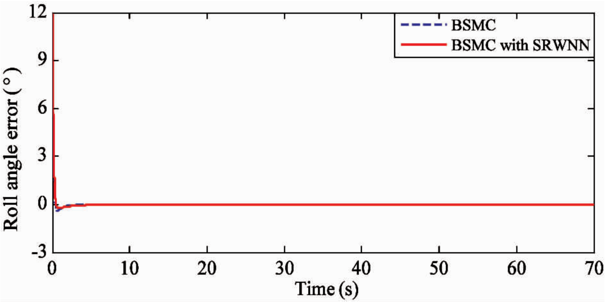

(a) Roll angle error under model uncertainties

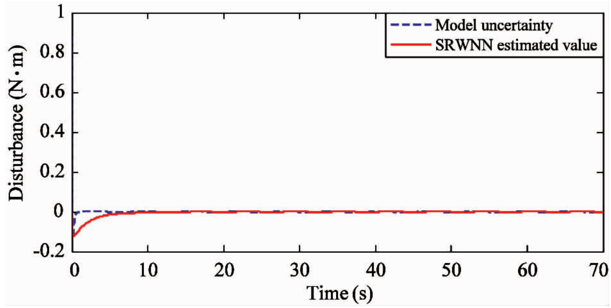

(b) SRWNN observed result under model uncertainties

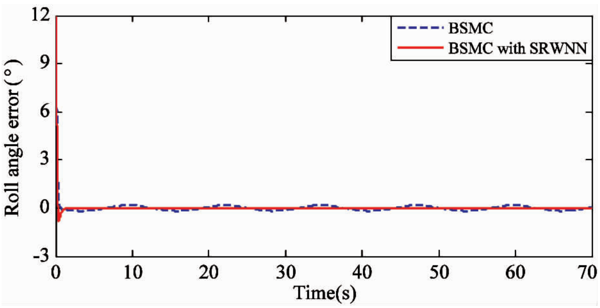

(c) Roll angle error under external disturbance

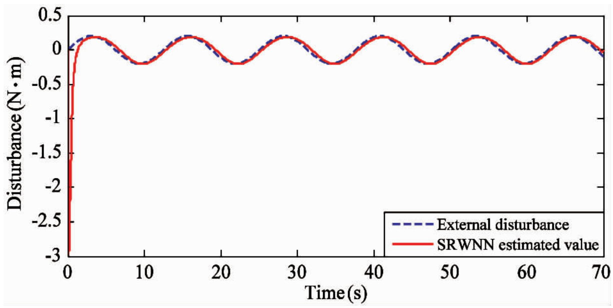

(d) SRWNN observed result under external disturbance

Fig. 4 The roll control comparison result under uncertainties

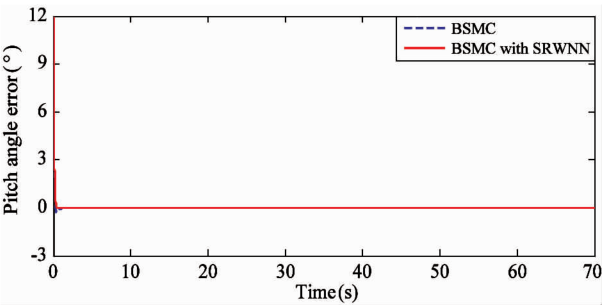

(a) Pitch angle error under model uncertainties

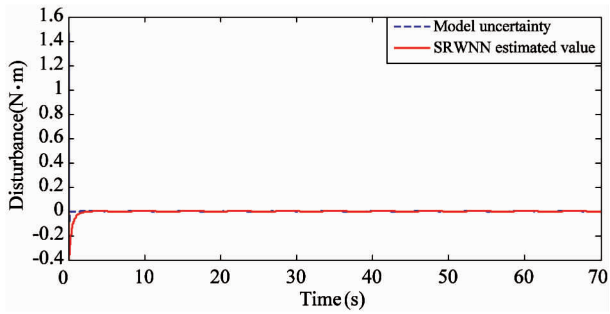

(b) SRWNN observed result under model uncertainties

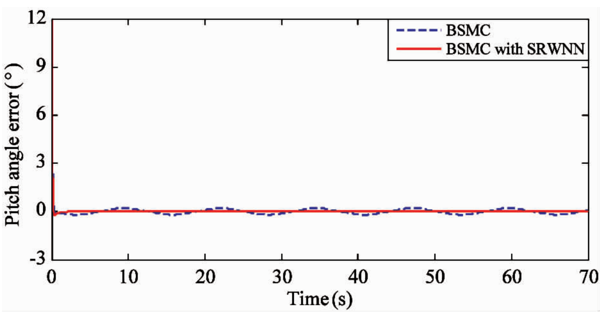

(c) Pitch angle error under external disturbance

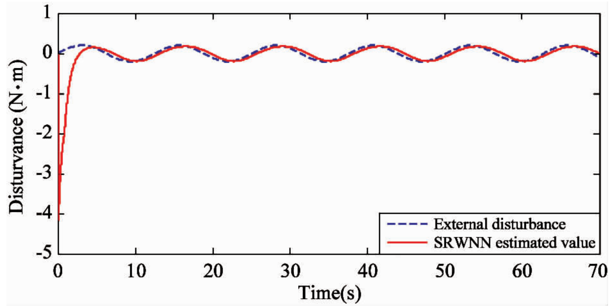

(d) SRWNN observed result under external disturbance

Fig. 5 The pitch control comparison result under uncertainties

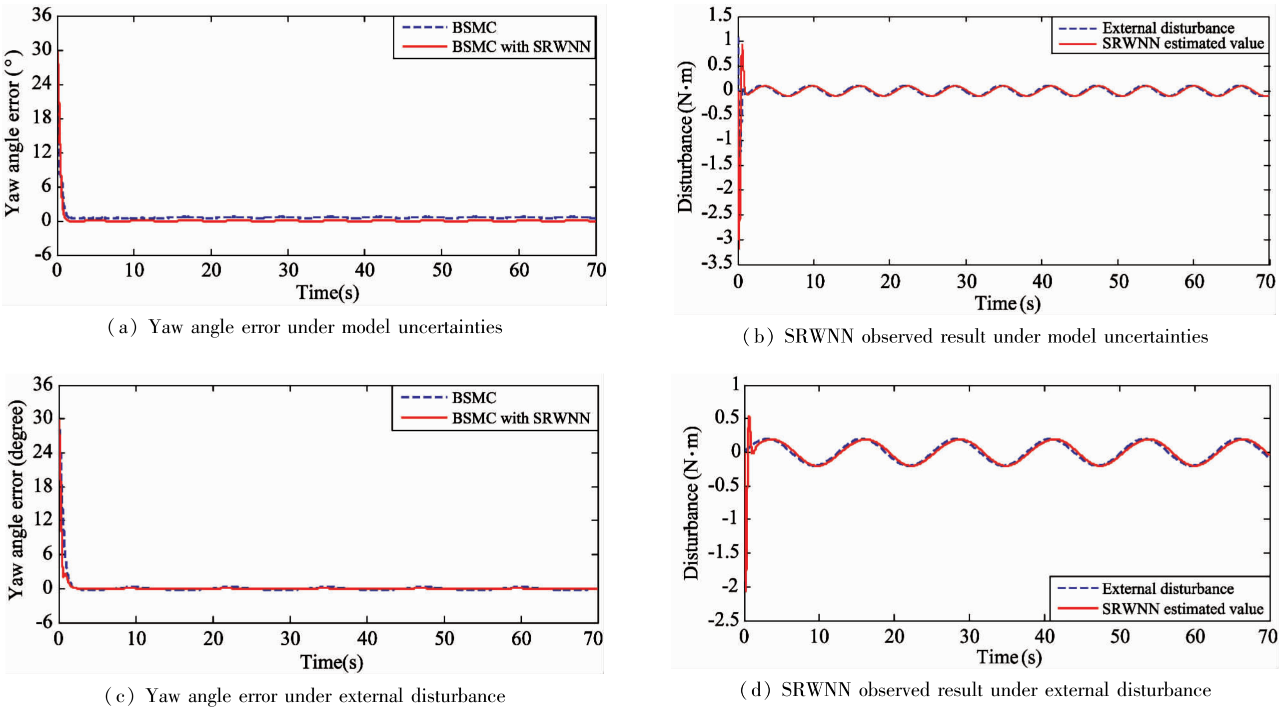

(a) Yaw angle error under model uncertainties

(b) SRWNN observed result under model uncertainties

(c) Yaw angle error under external disturbance

(d) SRWNN observed result under external disturbance

Fig. 6 The yaw control comparison result under uncertainties

It can be noted that the proposed method provides much greater control performance than BMSC method, which is more obvious under external disturbances. In addition, the SRWNN observer has the satisfied uncertainties estimation performance. Therefore, attitude compared simulation results highlight the claim that BSMC with SRWNN method possesses more favorable attitude control performance and much stronger robustness than BSMC method in the case of model uncertainties and external disturbances. It is clear that the proposed method is better suited in dealing with the robust control problem about the twelve-rotor UAV with uncertainties.

4 Prototype experiment results

4.1 Experimental setup

The twelve-rotor prototype designed with military grade carbon fiber is shown in Fig. 7, it has six pairs of blades driven by twelve brushless direct current (BLDC) motors mounted at each end of body frame. The schematic view of aerial control platform is presented in Fig. 8, which uses TMS320F28335 DSP that runs at 150MHz with 512K flash memory, including 12-bit analog input and 16 channels with programmable gains, as well as supports floating point calculations as the on-board flight control computer. An inertial measurement unit (IMU) including gyroscopes, accelerometers, magnetometers and the distance laser sensor is installed on the prototype to measure flight states. The sensor dates can be transmitted to the on-board flight control computer through an RS232 serial port. Then, the on-board computer can export these dates through wireless transfer module to the host computer that will generate the corresponding schematic diagrams.

Fig. 7 The twelve-rotor prototype

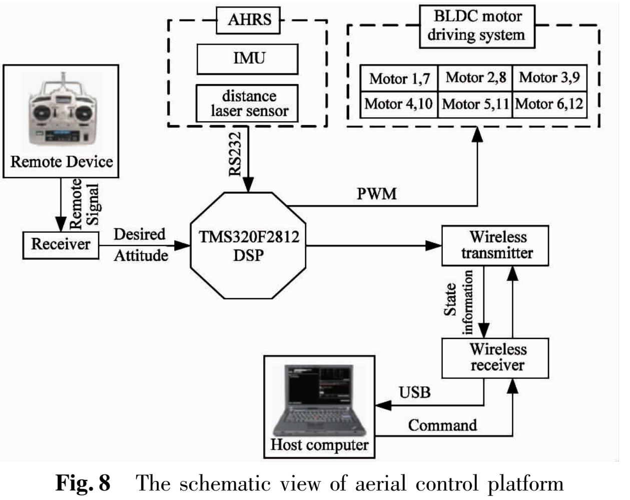

Fig. 8 The schematic view of aerial control platform

4.2 Experimental results

The validity and robustness are verified by the twelve-rotor prototype experiments based on BSMC with SRWNN method. The parameters of the controller are the same as those in simulations. The three desired attitude angles are given by the operator with remote device manually. The attitude angle tracking results are shown in Fig. 9, Fig. 10 and Fig. 11, in which it can be clearly noted that BSMC with SRWNN method can offer the great attitude control performance. It is obtained that the proposed method is well suited in dealing with the robust control problem about the twelve-rotor UAV.

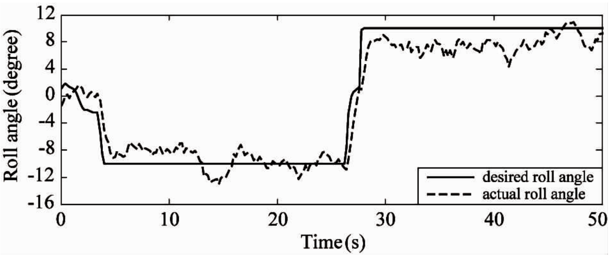

Fig. 9 The roll angle tracking result

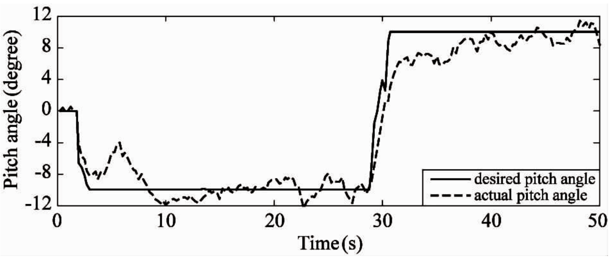

Fig. 10 The pitch angle tracking result

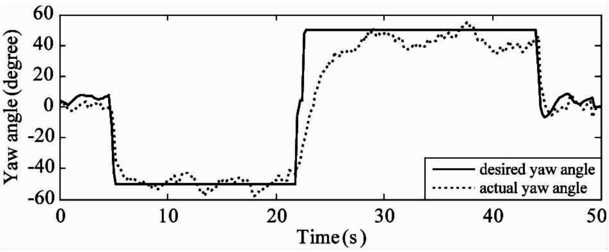

Fig. 11 The yaw angle tracking result

5 Conclusion

In this paper, a novel coaxial twelve-rotor UAV is designed with greater drive capacity and the decoupling on movement and attitude. On account of robust attitude control problem, the BSMC with SRWNN control strategy is proposed as the attitude controller of the twelve-rotor with uncertainties. The combination between backstepping control and sliding mode control has simplified design procedure and increasing robustness. The SRWNN observer is able to estimate lumped uncertainties effectively. Finally, simulation experiments demonstrate BSMC with SRWNN method applied to twelve-rotor can provide the favorable attitude control performance and strong robustness in the case of model uncertainties and external disturbances. Meanwhile, the validity of the proposed method is verified again via coaxial twelve-rotor prototype experiments.

References

[1] Ricardo P A, Javier M V, Roger M C. A robust approach for trajectory tracking control of a quadrotor with experimental validation[J]. *ISA Transactions*, 2016, 65: 262-274

[2] Dario M, Javier d L, Juan P F. Vision-based anticipatory controller for the autonomous navigation of an UAV using artificial neural networks [J]. *Neurocomputing*, 2015, 151: 101-107

[3] Chen Z J, Zhang R L, Zhang P, et al. Flight control: chanllenges and opportunities[J]. *Acta Automatica Sinica*, 2013, 39(6): 703-710

[4] Mohammadi M, Shahri A M. Adaptive nonlinear stabilization control for a quadrotor UAV: theory, simulation and experimentation[J]. *Journal of Intelligent & Robotic Systems*, 2013, 72(1): 105-122

[5] Ryan T, Kim H J. LMI-based gain synthesis for simple robust quadrotor control[J]. *IEEE Transactions on Automation Science and Engineering*, 2013, 10(4): 1173-1178

[6] Derafa L, Benallegue A, Fridman L. Super twisting control algorithm for the attitude tracking of a four rotors UAV [J]. *Journal of the Franklin Institute*, 2012, 349 (2): 685-699

[7] Yeh F K. Attitude controller design of mini-unmanned aerial vehicles using fuzzy sliding-mode control degraded by white noise interference[J]. *IET Control Theory & Applications*, 2012, 6 (9): 1205-1212

[8] Ku C C, Lee K Y. Diagonal recurrent neural networks for dynamic systems control[J]. *IEEE Transactions on Neural Networks*, 1995, 6(1): 144-156

[9] Zhang Q H, Benveniste A. Wavelet networks[J]. *IEEE Transactions on Neural Networks*, 1992, 3(6): 889-898

[10] Yoo S J, Park J B, Choi Y H. Adaptive dynamic surface control of flexible-joint robots using self-recurrent wavelet neural network[J]. *IEEE Transactions on Systems, Man, and Cybernetics*, 2006, 36(6):1342-1355

[11] Slotine J J E, Li W P. Applied Nonlinear Control[M]. New York: Prentice-Hall, 1991. 224-228

Qiao Guanyu, born in 1987. He is a Ph. D candidate in Changchun Institute of Optics, Fine Mechanics and Physics, Chinese Academy of Sciences. He received his M. S. degree in Machinery and Electronics Engineering of University of Chinese Academy of Sciences in 2013. He also received his B. S. degree from Jilin University in 2010. His research interests include the modeling and control of robots, robot force control.